GKAP-DLC2 interaction organizes the postsynaptic scaffold complex to enhance synaptic NMDA receptor activity

Enora Moutin, F. Raynaud, Laurent Fagni, Julie Perroy

GKAP–DLC2 interaction organizes the postsynaptic scaffold complex to enhance synaptic NMDA receptor activity

Enora Moutin[1,2,3], Fabrice Raynaud[1,2,3], Laurent Fagni[1,2,3] and Julie Perroy[1,2,3,*]

[1]CNRS, UMR-5203, Institut de Génomique Fonctionnelle, F-34000 Montpellier, France
[2]INSERM, U661, F-34000 Montpellier, France
[3]Universités de Montpellier 1 and 2, UMR-5203, F-34000 Montpellier, France
*Author for correspondence (julie.perroy@igf.cnrs.fr)

Summary

At glutamatergic brain synapses, scaffolding proteins regulate receptor location and function. The targeting and organization of scaffolding proteins in the postsynaptic density (PSD) is poorly understood, but it is known that a core protein of the glutamatergic receptor postsynaptic scaffold complex, guanylate-kinase-associated protein (GKAP) interacts with dynein light chain 2 (DLC2, also known as DYNLL2), a protein associated with molecular motors. In the present study, we combined BRET imaging, immunostaining and electrophysiological recording to assess the role of the GKAP–DLC2 interaction in the functional organization of the glutamatergic synapse. We found that GKAP–DLC2 interaction in dendritic spine stabilizes scaffolding protein expression at the PSD and enhances synaptic NMDA receptor activity. Moreover, the GKAP–DLC2 functional interaction is favored by sustained synaptic activity. These data identify a regulatory pathway of synaptic transmission that depends on activity-induced remodelling of the postsynaptic scaffold protein complex.

Key words: Dynein light chain, Guanylate-kinase-associated protein, BRET imaging, Scaffolding proteins, Synaptic transmission

Introduction

Electron microscopic analysis of glutamatergic synapses revealed an electron-dense organelle, right beneath the postsynaptic membrane, which was named postsynaptic density (PSD) (Palay, 1958). The PSD consists of a network of proteins that anchor and link glutamate receptors and other postsynaptic proteins to the cytoskeleton and signaling pathways (Ehlers et al., 1996; Kennedy, 1997; Scannevin and Huganir, 2000; Sheng and Pak, 2000). Changes in PSD scaffolding protein integrity can influence excitatory synaptic transmission through glutamate receptor redistribution and signaling (Ehrlich and Malinow, 2004; Stein et al., 2003). The guanylate-kinase-associated protein [GKAP; also known as synapse-associated 42 protein 90-postsynaptic density-95-associated protein (SAPAP) and Discs-large-associated 43 protein (DAP) family proteins] is highly enriched and specifically localized in the PSD. There are at least four alternative splicings of the GKAP gene (Kim et al., 1997). GKAP proteins bind the guanylate kinase-like domain of postsynaptic density protein 95 (PSD-95) (Kim et al., 1997; Naisbitt et al., 1997; Takeuchi et al., 1997), synaptic scaffolding molecule (S-SCAM) (Hirao et al., 1998) and PSD-95–Discs large–zona occludens-1 (PDZ) domains of shank1–3 proteins (Boeckers et al., 1999; Naisbitt et al., 1999). GKAP binding to Shank proteins is mediated by a short C-terminal sequence common to all GKAP splice variants, whereas its binding to PSD-95 is mediated by the N-terminal region, which contains five repeats of 14 amino acids highly conserved in all GKAP proteins (Kim et al., 1997). By interacting with PSD-95 and Shank, GKAP physically links the N-methyl-D-aspartic acid (NMDA) receptor–PSD-95 complex to the type I metabotropic glutamate receptor–Homer complex (Naisbitt et al., 1999; Tu et al., 1999). GKAP is therefore one of the major scaffold proteins organizing glutamate receptors in the PSD. The molecular mechanisms regulating the post-synaptic targeting and assembly of neurotransmitter receptors and associated scaffolding proteins in the PSD are still largely unknown. Indeed, PSD-95 seems to be involved in NMDA clustering (Kornau et al., 1995; Niethammer et al., 1996), whereas GKAP could be involved in the modulation of the NMDA receptor-channel activity through PSD-95 (Yamada et al., 1999).

A few years ago, Naisbitt et al. (Naisbitt et al., 2000) identified a new GKAP interactor, dynein light chain (DLC; also known as DYNLL and LC8), a light chain that is shared by cytoplasmic dynein and myosin-V (Benashski et al., 1997). This adaptor protein functions as a molecular motor that drives the trafficking of cargoes along microtubules and actin filaments. DLC is an 8 kDa protein that is highly conserved from rice to human (King et al., 1996; King and Patel-King, 1995) and it is ubiquitously expressed in organisms. In mammals, there are two DLC isoforms, DLC1 and DLC2. Its crucial role has been demonstrated in several organisms, including *Drosophila*, in which null mutations result in embryonic lethality (Dick et al., 1996). DLC associates with a wide variety of proteins, including neuronal nitric oxide synthase (nNOS) (Jaffrey and Snyder, 1996), gephyrin (Fuhrmann et al., 2002), bassoon (Fejtova et al., 2009), the proapoptotic factor Bim (Puthalakath et al., 1999), transcriptional factors Swallow (Schnorrer et al., 2000) and Trps1

(Kaiser et al., 2003), viral proteins (Raux et al., 2000) and p53 binding protein 1 (Lo et al., 2005). Because DLC is a light chain of motor proteins, its role in trafficking has been widely assessed. Thus DLC has been reported to link cargoes to the molecular motors (Lee et al., 2006; Navarro et al., 2004; Schnorrer et al., 2000). In 2008, Elisar Barbar proposed that DLC is an essential Hub protein in various protein networks (Barbar, 2008). Indeed, a large number of studies suggested involvement of DLC in many biological processes such as in viral and RNA transport (Raux et al., 2000), apoptosis (Puthalakath et al., 1999; Puthalakath et al., 2001), cell cycle (Lo et al., 2005; Vadlamudi et al., 2004), inhibition of nNOS (Jaffrey and Snyder, 1996), facilitation of Swallow folding (Schnorrer et al., 2000), macropinocytosis (Yang et al., 2005) and nuclear transport (Sodeik et al., 1997). Dimerization of DLC (Benashski et al., 1997) is required for its activity (Wang et al., 2003). Moreover, it has been observed in several cases that DLC interacts with partially disordered proteins and promotes their dimerization (Barbar, 2008).

Because GKAP is a core protein of the glutamate receptor complex, its association with DLC2 might be important in the targeting and organization of the receptors and associated scaffolding proteins in dendritic spines. It is therefore essential to understand the spatiotemporal dynamics of the GKAP–DLC2 interaction and its function in glutamate receptor activity. We have identified the molecular determinants involved in the GKAP–DLC2 interaction. We further investigated, by single cell bioluminescence resonance energy transfer (BRET) imaging, the spatiotemporal dynamics of this interaction in cultured hippocampal neurons and its consequences on NMDA receptor function. We found that GKAP–DLC2 interaction was prominent in dendritic spines and could be further increased by sustained synaptic activity. This GKAP–DLC2 interaction enabled the accumulation of GKAP and PSD-95 in dendritic spines and potentiated synaptic NMDA currents.

Results

GKAP interacts with DLC2 in living cells

To assess the occurrence of GKAP–DLC2 interaction in a physiological context by bioluminescence resonance energy transfer (BRET), we fused the N-terminus of GKAP to the energy donor *Renilla* luciferase (RLuc8) and the N-terminus of DLC2 to the acceptor yellow fluorescent protein, Venus (RLuc8–GKAP and Venus–DLC2). Addition of the tag did not impair the known properties of these proteins: RLuc8–GKAP interacted with PSD-95 and Shank3 (supplementary material Fig. S1A) and Venus–DLC2 was able to form dimers (supplementary material Fig. S1B). In hippocampal neurons, these two tagged proteins were ubiquitously expressed and colocalized in dendritic spines of cultured hippocampal neurons (Fig. 1A).

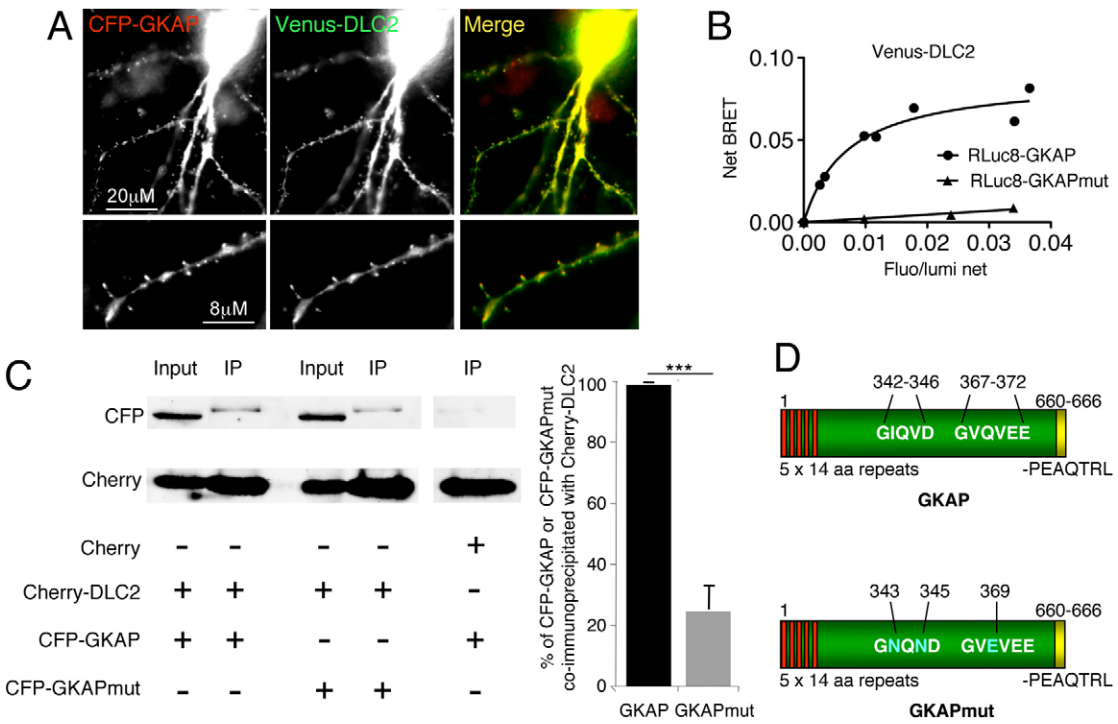

Fig. 1. GKAP interacts with DLC2 in living cells. (**A**) Localization of CFP–GKAP and Venus–DLC2 in DIV14 hippocampal neurons. (**B**) HEK293 cells were co-transfected with constant concentrations of RLuc8–GKAP or RLuc8–GKAPmut and increasing concentrations of Venus–DLC2 expression plasmids. BRET was expressed as a function of the Venus–DLC2 acceptor expression level. Individual readings obtained from three independent experiments were pooled. Curves were fitted using a nonlinear regression equation (GraphPadPrism), assuming a single binding site. (**C**) HEK293 cells were co-transfected with mCherry–DLC2 and CFP–GKAP or CFP–GKAPmut expression plasmids. mCherry–DLC2 was immunoprecipitated with RFP–Trap and the amount of CFP–GKAP or CFP–GKAP mutant co-immunoprecipitated was quantified by western blot analysis using the anti-GFP antibody. The control assay was performed under the same conditions but with mCherry instead of mCherry–DLC2 (last column). For the immunoprecipitations (IPs), the ratio of CFP–GKAPmut/mCherry–DLC2 was expressed as a percentage of the ratio of CFP–GKAP/mCherry–DLC2. Values are means ± s.e.m. of three individual experiments [***significantly different ($P<0.001$), Mann–Whitney *U*-test]. (**D**) Schematic representations of GKAP and GKAPmut. The putative GKAP amino acid sequences for binding to DLC2 are indicated in white; mutations engineered to obtain GKAPmut are indicated in blue.

When expression of RLuc8–GKAP was constant, the BRET signal increased hyperbolically as a function of the Venus–DLC2 expression level (Fig. 1B). Saturation of the BRET signal when all the donor was linked to the acceptor indicated a specific interaction between GKAP and DLC2 proteins. This interaction was further confirmed by co-immunoprecipitation (Fig. 1C). We assessed by BRET whether DLC2 could also bind other PSD-associated scaffolding elements. None of the proteins tested (PSD95, Shank3 and Homer3) produced a specific BRET signal with DLC2, indicating specificity of binding of DLC2 to GKAP (supplementary material Fig. S1C).

To characterize the molecular determinants involved in the interaction of GKAP with DLC2, we screened the amino acid sequences of other DLC2 interactors and found two conserved consensus binding sites: GIQVD and GVQVEE (Lajoix et al., 2004; Lo et al., 2001; Navarro-Lérida et al., 2004). The glycine residue as well as the −1 and +1 flanking amino acids might be crucial for the interaction (Lajoix et al., 2004). Accordingly, using molecular biology we produced a cDNA coding for a GKAP mutant in which GIQVD and GVQVEE were mutated to GNQND and GVEVEE, respectively (GKAPmut; Fig. 1D). BRET and co-immunoprecipitation experiments detected a loss of interaction between GKAPmut and DLC2 (Fig. 1B,C). Taken together, these data showed that GKAP and DLC2 interacted in living cells and three point mutations on GKAP were sufficient to impair this interaction.

We further characterized the association between GKAP and DLC2 at the subcellular level by imaging protein–protein interactions on single hippocampal neuron using BRET imaging (Coulon et al., 2008; Perroy, 2010). The BRET signal between RLuc8–GKAP and Venus–DLC2 was homogeneous in the cell body and punctiform in dendrites (Fig. 2A). The mean BRET intensity was significantly higher in dendrites than in soma (124.5±4.2 and 99.8±1.8, respectively; $P<0.01$; Fig. 2B, left) and importantly, the standard deviation was almost three times higher for dendrites than soma (80.3±2.4 and 22.4±2.3, respectively; Fig. 2B, right), which was consistent with a higher punctiform distribution in the dendrites than in soma.

Neuronal activity potentiates GKAP–DLC2 interaction

We next analyzed the effect of neuronal activity on GKAP–DLC2 interaction. To enhance neuronal activity, we used a specific blocker of transient outward voltage-dependent potassium currents, 4-AP (1 mM) (Buckle and Haas, 1982). BRET signal between RLuc8–GKAP and Venus–DLC2 in hippocampal neurons was recorded before and during 4-AP exposure (Fig. 3A). After 4-AP exposure, the mean BRET signal increased in soma (109.33±3.13% at 10 minutes; $n=21$) and dendrites (111.96±3.39% at 10 minutes; $n=21$; Fig. 3B). The standard deviation increased in soma (155.06±11.41%; $n=21$; Fig. 3C), suggesting an important clustering of GKAP–DLC2 complex induced by 4-AP application. In dendrites, the standard deviation also significantly increased after 4-AP application, but to a lesser extent (104.11±1.21%; $n=21$; $P<0.01$; Fig. 3C), probably because of an already important basal clustering (Fig. 2B). Indeed, despite the strong increase in the soma, the BRET signal standard deviation remained higher in dendrites

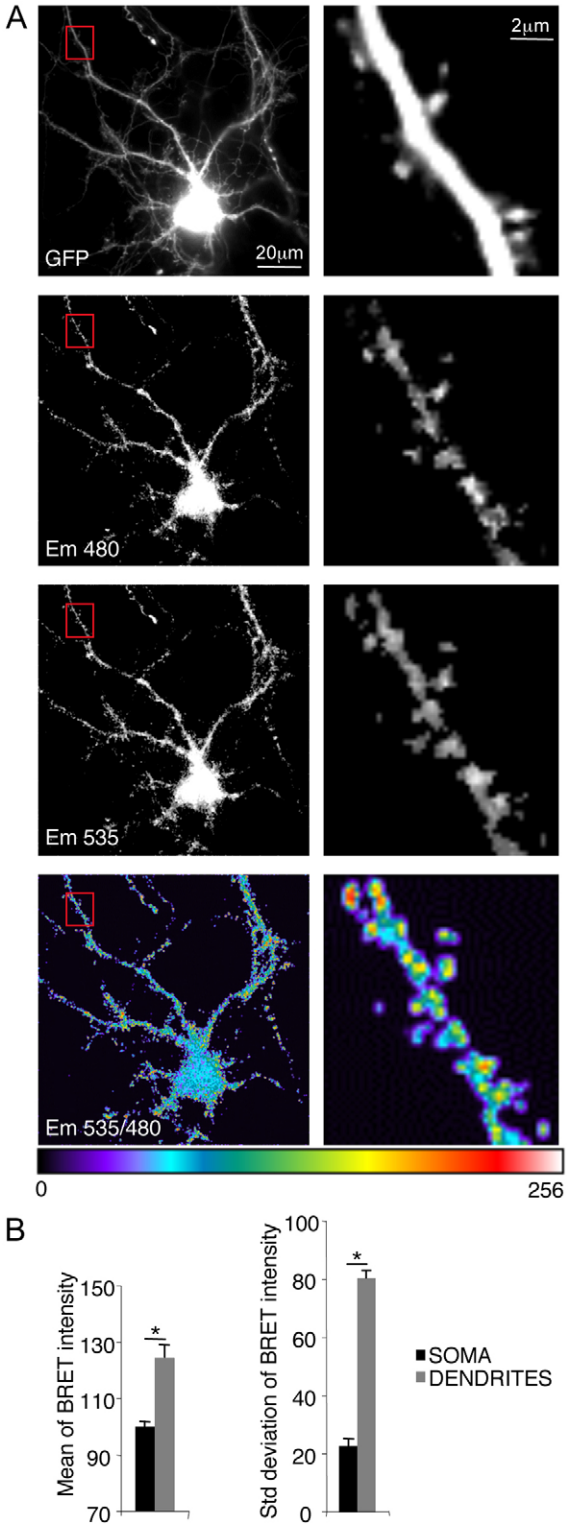

Fig. 2. GKAP interacts with DLC2 in neurons. (**A**) Neurons were co-transfected with RLuc8–GKAP and Venus–DLC2 and BRET was imaged in a 20 × 20 μm area in the dendrites. The pictures show expression of Venus-DLC2 (GFP), RLuc8–GKAP (Em480), Venus-DLC2 excited by energy transfer (Em535) and BRET signal generated by the two tagged proteins (535/480). The regions boxed in red are shown at a higher magnification in the panels on the right. (**B**) BRET intensity. (Left) Intensity in dendrites and soma. Note that higher BRET signals were found in the dendrites than in the cell bodies. (Right) The standard deviation of the BRET intensity in dendrites and soma. Note that a high standard deviation indicates a clustering in dendrites [$n=6$ neurons; *significantly different ($P<0.01$), Wilcoxon test].

than in soma after 4-AP stimulation (absolute mean BRET values: 32.4±2.6 in soma and 86.5±1.1 in dendrites). The observed activity-dependent increase in BRET intensity and standard deviation in dendrites might be due to an increase in BRET in dendritic spines. Consistent with this hypothesis, BRET intensity was measured in dendritic spines specifically, where we found a significant increase after 4-AP exposure (128.78±7.63% increase; $P<0.01$; 10 minutes after 4-AP application compared with control; $n=72$ spines; Fig. 3D). A similar modulation of DLC2–GKAP interaction could be obtained by stimulation of postsynaptic NMDA receptors with a specific agonist (supplementary material Fig. S2). These experiments highlighted a neuronal activity-induced potentiation of GKAP–DLC2 interaction in postsynaptic elements.

In addition, we noticed that the BRET signal was different between spines. These differences might reflect physiological disparities between spines such as different amount of proteins per spine. Because the BRET signal between GKAP and DLC2 depends on the DLC2 and GKAP expression ratio, small differences in protein expression in the spine would influence the level of BRET. More importantly, spines are particularly advantageous for neurons because they compartmentalize biochemical and electrical signals. This can help to encode changes in the state of an individual synapse without necessarily affecting the state of other synapses of the same neuron. The neuronal activity is not homogeneous but varies from one spine to another. The observed differences in BRET signal between spines were therefore consistent with, and reinforced, the idea that synaptic activity regulates the interaction between DLC2 and GKAP in spines.

GKAP–DLC2 interaction enables a synaptic activity-dependent accumulation of GKAP in dendritic spines

Because 4-AP increased GKAP–DLC2 interaction in spines, we studied in more detail the consequences of neuronal activity on CFP–GKAP accumulation in dendritic spines (Fig. 4A). To this aim, we measured the ratio of fluorescence intensity in dendritic spines to the intensity in dendritic shafts, before and during 4-AP application. Before 4-AP application, the spine/shaft fluorescence ratio was 2.4, indicating a preferential expression of GKAP in the spine, under basal conditions. Interestingly, after 5 minutes of 4-AP application, CFP–GKAP spine/shaft fluorescence intensity increased by 32.9±9.2%, thus highlighting an activity-dependent increase of GKAP protein in dendritic spines (Fig. 4B). To assess the role of GKAP–DLC2 interaction in the accumulation of GKAP in spine, we used the CFP–GKAPmut construct that did not interact with DLC2 (Fig. 1). The synaptic localization of CFP–GKAPmut was significantly ($P<0.001$) reduced (−16.4%) compared with CFP–GKAP, but its spine/shaft fluorescence ratio was still greater than one, suggesting that although interaction with DLC2 could modulate spine-preferential localization of

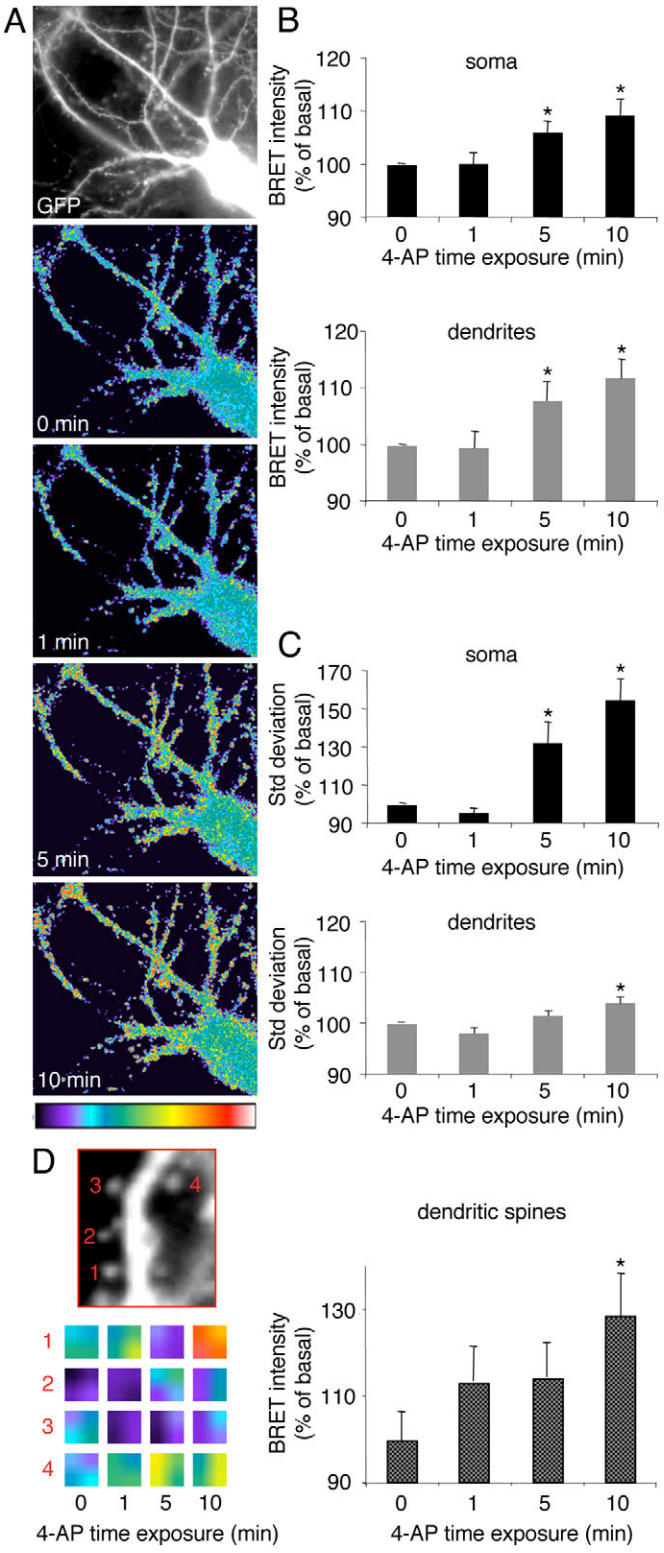

Fig. 3. Neuronal activity potentiates GKAP–DLC2 interaction. (**A**) Neurons were co-transfected with RLuc8–GKAP and Venus–DLC2. The images show expression of Venus–DLC2 (GFP) and BRET signal generated by the two-tagged proteins (535/480) following exposure to 4-AP (1 mM). (**B**) BRET intensity at different times after 4-AP treatment (percentage of basal signal), in soma and dendrites. (**C**) The standard deviation of BRET intensity after 4-AP treatment (% of the basal signal), in soma and dendrites (in B and C values are means ± s.e.m., $n=21$ neurons, from four independent experiments). (**D**) Left: example of BRET signals in four dendritic spines during 4-AP stimulation. Note that the strong dynamic of the protein–protein interaction in this area makes the BRET signal vary from one spine to another. Right: BRET intensity at different times during 4-AP treatment (percentage of the basal signal), in dendritic spines (values are means ± s.e.m., $n=72$ spines, from 17 neurons in four independent experiments; *significantly different ($P<0.01$), Student's t-test.

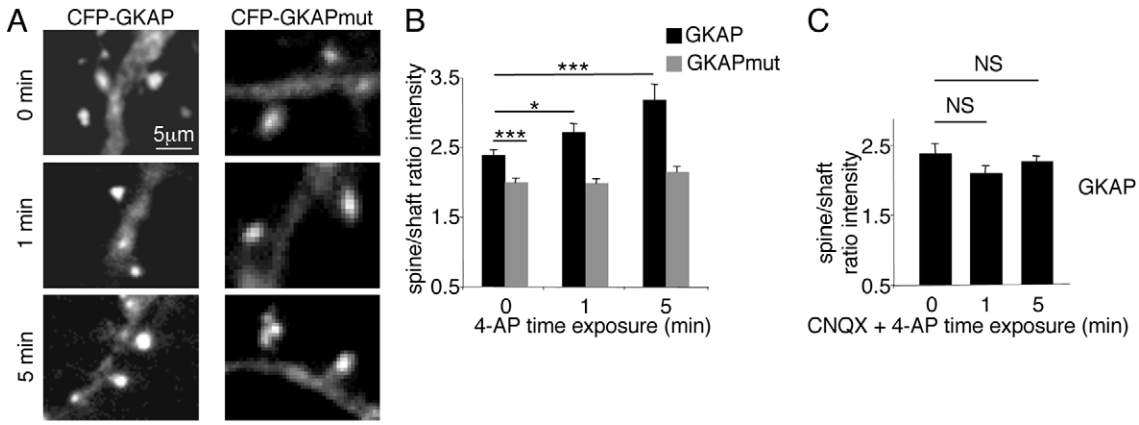

Fig. 4. GKAP–DLC2 interaction enables a synaptic activity-dependent accumulation of GKAP in dendritic spines. (**A**) Expression and location of CFP–GKAP or CFP–GKAPmut in neurons stimulated with 4-AP (1 mM). (**B**) The spine/shaft fluorescence ratio of neurons transfected with CFP–GKAP (black) or CFP–GKAPmut (grey) after 4-AP (1 mM) treatment. (**C**) The spine/shaft fluorescence ratio of neurons transfected with CFP–GKAP following treatment with 4-AP (1 mM) + CNQX (10 µM). For B and C, values are means ± s.e.m. of three independent experiments, 10 neurons per experiment, 10 spines per neuron. Significant differences: *$P<0.01$ and ***$P<0.001$, Student's *t*-test; NS, not significant.

GKAP, this interaction was not essential in basal conditions. In contrast to GKAP, the fluorescence intensity of the GKAPmut was not significantly ($P<0.01$) modulated by 4-AP application, suggesting that GKAP–DLC2 interaction was necessary for activity-induced GKAP accumulation in spines (Fig. 4B). In contrast to GKAP, DLC2 content in the post-synaptic compartment was not modulated by 4-AP treatment (supplementary material Fig. S3), suggesting that the activity regulates only GKAP in a DLC2 interaction-dependent manner. The 4-AP-induced GKAP accumulation in spines was blocked by co-application of 6-cyano-7-nitroquinoxaline-2,3-dione (CNQX; Fig. 4C), a competitive AMPA and kainate antagonist, indicating that 4-AP-induced increase in GKAP accumulation in spines was mediated by elevated synaptic activity rather than intrinsic neuronal activity per se. Interestingly, co-expression of DLC2 abolished the relocation of GKAP in spines by this activity (supplementary material Fig. S4). The overexpression of light chains is known to prevent the correct association of molecular motor complex and can indeed be used as a dominant-negative tool causing the molecular motor complex to dissociate and decoupling the motor from its cargo (see Echeverri et al., 1996). In this condition GKAP expression is no longer enhanced in spines upon neuronal activity. To summarize, GKAP–DLC2 interaction enabled trafficking and accumulation of GKAP in dendritic spines and this effect was promoted by sustained synaptic activity.

GKAP–DLC2 interaction modulates the synaptic localization of PSD-95

Because GKAP is a core protein of the postsynaptic glutamatergic receptor complex, we further studied GKAP–DLC2 interaction in the accumulation of GKAP scaffold partners in the dendritic spine. We assessed the spine/shaft fluorescence ratio of PSD-95–YFP, Venus–Shank3, Venus–Homer3 or Venus–GIT1 (G-protein-coupled receptor kinase interacting protein 1; a multifunctional adaptor protein expressed in dendrites) when coexpressed with GKAP or GKAPmut (Fig. 5A), a construct that still interacted with Shank3 and PSD-95 (supplementary material Fig. S5), but not DLC2 (Fig. 1). We found that GKAP induced a significant ($P<0.01$) increase in the Shank3 (15.2%±6.6), Homer3 (18.4%±4.4) and PSD-95 (52.6±8.0%) but not GIT1 spine/shaft fluorescence ratio. None of these expression ratios was affected by the presence of GKAPmut. This differential effect of GKAP and GKAPmut highlighted the importance of the GKAP–DLC2 complex in the preferential location of GKAP partners in the spine. The observed PSD-95 accumulation in the spine, induced by the GKAP–DLC2 interaction, could be explained by GKAP targeting and trafficking of the PSD-95–GKAP–DLC2 complex to the spine, or stabilization of PSD-95 by the GKAP–DLC2 complex in the spine. To further discriminate between the role of GKAP accumulation per se and its interaction with DLC2 in PSD-95 accumulation in spine, we studied PSD-95 spine/shaft localization ratio as a function of GKAP or GKAPmut expression level (Fig. 5B). The preferential localization of PSD-95 in spines increased as a function of GKAP, but not GKAPmut expression level (Fig. 5B). The absence of correlation between GKAPmut expression level and PSD-95 preferential localization in spines suggested that local interaction of GKAP with DLC2, rather than accumulation of GKAP per se stabilized PSD-95 in spines.

Because neuronal activity increased GKAP–DLC2 interaction in spines, we examined whether this also applied to PSD-95 accumulation. Application of 4-AP for 5 minutes indeed stably increased accumulation of PSD-95 in spines (Fig. 5C). Consistent with the hypothesis that neuronal activity-induced PSD-95 accumulation relied on GKAP accumulation in spines, transfection of GKAP increased the basal PSD-95 accumulation in spines (as previously shown, Fig. 5A), but precluded an additional effect of sustained neuronal activity on PSD-95 accumulation in dendritic spines (Fig. 5C). Furthermore, although the PSD-95 spine/shaft ratio was not significantly ($P<0.01$) different when co-transfected with CFP or CFP–GKAPmut in the basal condition (Fig. 5A), 4-AP application failed to increase PSD-95 accumulation in spines in the presence of GKAPmut (Fig. 5C). Taken together, these experiments suggested that GKAP–DLC2 interaction was responsible for

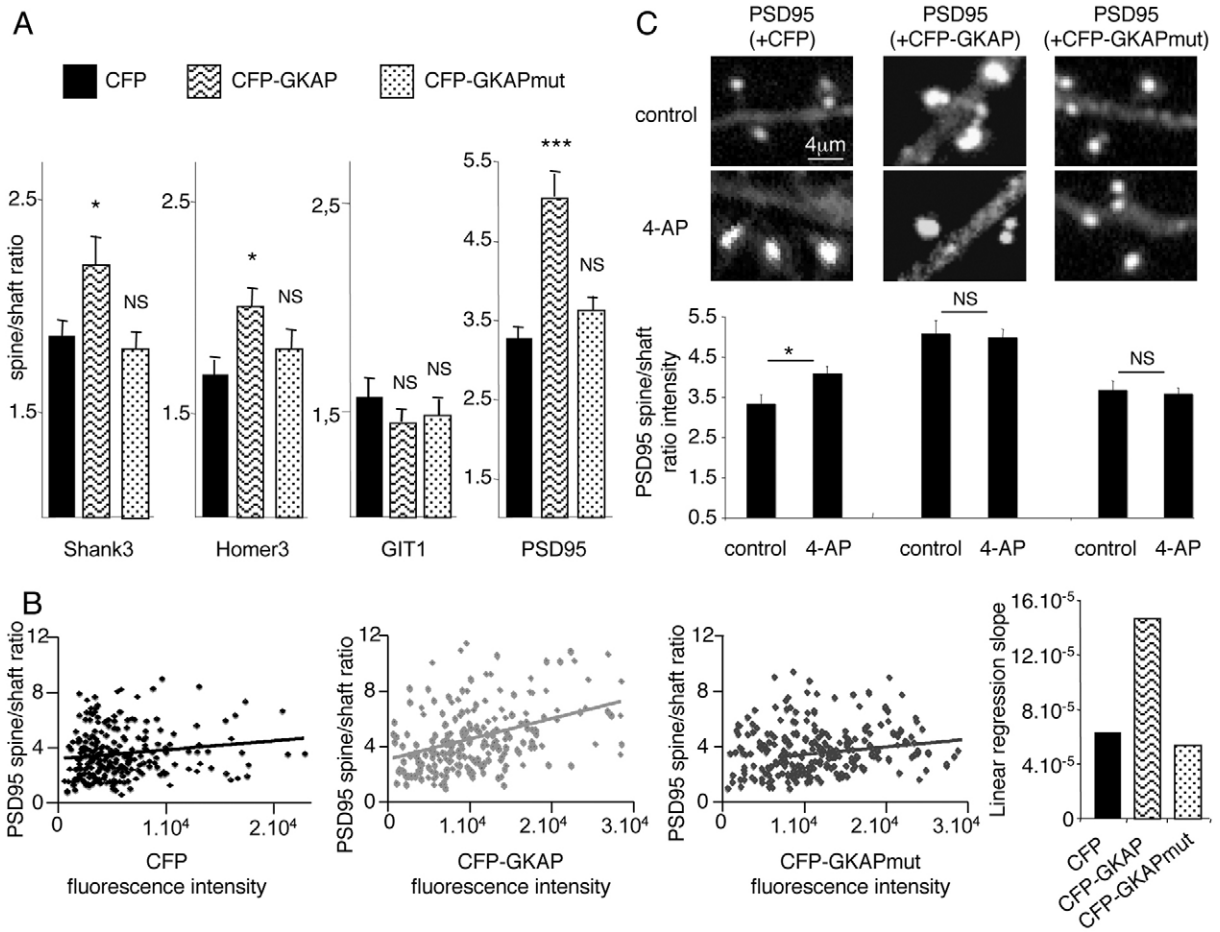

Fig. 5. GKAP–DLC2 interaction enhances the synaptic accumulation of PSD-95. (**A**) The spine/shaft fluorescence ratio of neurons transfected with Venus–Shank3 (left), Venus–Homer3 (middle left), Venus–GIT (middle right) or PSD-95-YFP (right). For each condition, neurons were co-transfected with either CFP (black), CFP–GKAP (waves) or CFP–GKAPmut (points). Each condition was compared with the CFP control. The statistical analysis was the same as in Fig. 4B. (**B**) Neurons were co-transfected with PSD-95–YFP and either CFP or CFP–GKAP or CFP–GKAPmut. The PSD-95 spine/shaft fluorescence ratio was expressed as a function of CFP or CFP–GKAP or CFP–GKAPmut expression level in spines. Each point of the scatter plots represents one spine. The histogram represents the slopes of the linear regression curves of the scatter plots. (**C**) Fluorescence images of PSD-95–YFP and histograms of the spine/shaft fluorescence ratio of PSD-95–YFP measured in neurons transfected with PSD-95–YFP and CFP (left) or CFP–GKAP (middle) or CFP–GKAPmut (right), before (control) and after 4-AP (1 mM) treatment. Note that the 4-AP treatment differs from that shown in previous figures: neurons were stimulated 5 minutes with 4-AP and then washed for 25 minutes before fixation to follow long lasting remodeling. The statistical analysis was the same as in Fig. 4B.

GKAP and PSD-95 accumulation in spines and this could be enhanced by neuronal activity. Note that the role of GKAP–DLC2 interaction in organizing the postsynaptic scaffold complex also applies to endogenous proteins, because endogenous PSD95 was re-located to spines upon neuronal activity in a GKAP–DLC2 interaction-dependent manner (supplementary material Fig. S6).

GKAP–DLC2 interaction enhances NMDA synaptic currents

Because GKAP–DLC2 interaction promotes synaptic localization of PSD-95, we investigated the modulatory role of this protein assembly on endogenous NMDA current. Neurons transfected with CFP–GKAP or CFP–GKAPmut were recorded in the whole-cell configuration using the patch-clamp technique and transiently perfused with NMDA. GKAP induced a 28.8±6.4% (n=24) increase in NMDA currents, whereas GKAPmut had no significant effect (11.8±8.6% decrease compared with the control; n=17). Downregulation of DLC2 by specific siRNA (supplementary material Fig. S7) abolished the GKAP-induced increase of NMDA currents (1.4±8.7% decrease compared with the control; n=9; Fig. 6A,B). These results suggest that GKAP expression potentiated NMDA currents through interaction of the protein with DLC2.

We further studied the modulatory action of the GKAP–DLC2 interaction on NMDA current at the synaptic level by analyzing the slow component of miniature excitatory postsynaptic currents (mEPSCs) carried by NMDA currents (Lu et al., 2001). The NMDA component was measured 7 mseconds after the peak amplitude of averaged mEPSCs, in untransfected neurons or neurons transfected with GKAP or GKAPmut. Overexpression of GKAP significantly (P<0.05) increased the amplitude of the synaptic NMDA component (synaptic NMDA current in the presence of GKAP: 130.9±9.0% of control condition; Fig. 6C). By contrast, GKAP mutant that could not interact with DLC2 had no significant effect on synaptic NMDA current (GKAPmut: 103.0±6.8% of synaptic NMDA current in control condition;

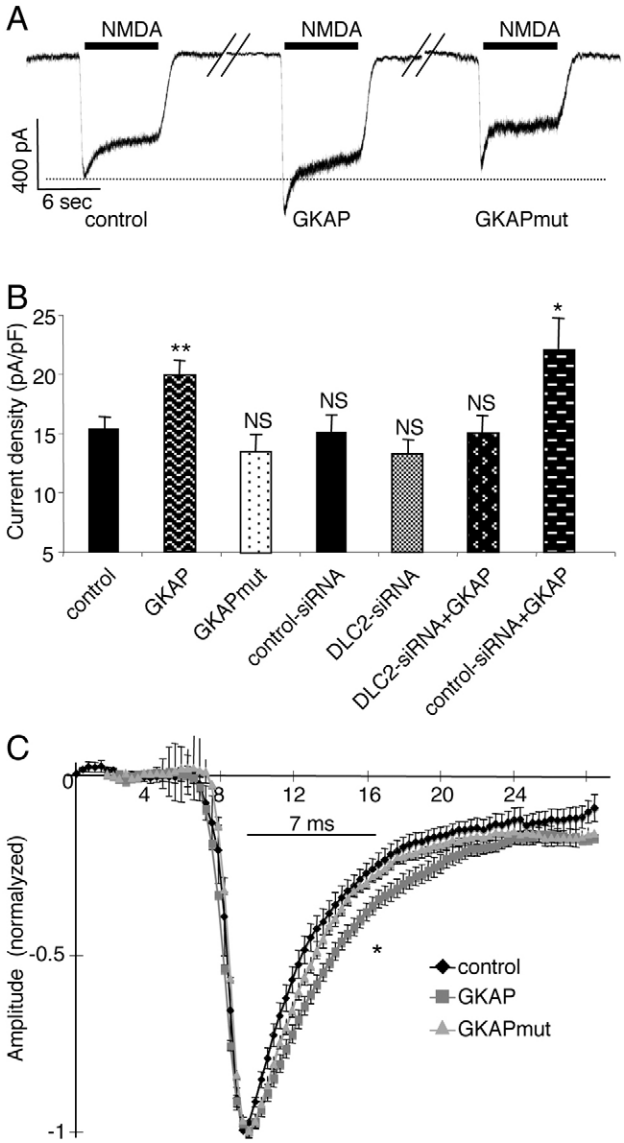

Fig. 6. GKAP–DLC2 interaction enhances NMDA synaptic currents. Neurons were transfected with Venus (control) and GKAP or GKAPmut, as indicated. (**A**) Representative traces of NMDA-induced current. Horizontal bars represent NMDA (100 μM) applications. (**B**) Each plot shows the means ± s.e.m. of NMDA current density from at least 10 neurons. Note that siRNAs were co-transfected with Venus as a transfection reporter. The statistical analysis was the same as in Fig. 4B; each condition was compared with the control. (**C**) Normalized averaged mEPSCs (>20) recorded from untransfected neurons or neurons transfected with GKAP or GKAPmut (=11 in each condition). The slow NMDA channel-mediated component of the mEPSCs was analyzed for 7 mseconds after the peak. *Significantly different ($P<0.05$), Mann–Whitney *U*-test.

Fig. 6C). These results highlight the potentiation of synaptic NMDA currents by GKAP, enhancement that requires the interaction of GKAP with DLC2.

Discussion

GKAP is a core protein of the scaffolding complex that governs glutamate receptor location and function in dendritic spines. Identification of the new GKAP interactor, DLC2, raised the question of its functional interaction in the organization and activity of the glutamate receptors. Using recent developments in single-cell BRET imaging (Coulon et al., 2008; Perroy, 2010), we have examined this issue by studying the spatiotemporal dynamics of GKAP–DLC2 interaction in living hippocampal neurons. We found that GKAP–DLC2 interaction was prominent in dendritic spines and could be increased by sustained synaptic activity. We identified the molecular determinant of the interaction, and engineered a GKAP mutant that lacked the ability to interact with DLC2. This allowed us to show that GKAP–DLC2 interaction activates accumulation of GKAP and PSD-95 in dendritic spines, and potentiates postsynaptic NMDA currents. Thus, a combination of BRET imaging, immunofluorescence staining and electrophysiological recording provided a better understanding of the physiological role of the GKAP–DLC2 complex in postsynaptic glutamate receptor assembly and function.

Our results showed that GKAP–DLC2 interaction favored preferential expression of GKAP in the spine. Because DLC2 is a light chain of myosin V, this adaptor protein might function as a molecular motor driving the specific trafficking of GKAP towards dendritic spines along actin filaments, up to the PSD. This would explain the essential role of the actin cytoskeleton in both maintenance and reorganization of the PSD (Kuriu et al., 2006). Accordingly, we found that GKAP–DLC2 interaction also affected the targeting of GKAP partners such as Shank3, Homer3 and PSD-95 to the spine. This extended role of the GKAP–DLC2 complex was consistent with previous findings documenting non-synaptic clusters of synaptic proteins (Gerrow et al., 2006). However, it is worth noting that PSD scaffolding proteins contain multiple binding motifs, and their interactions with other scaffolds and cytoskeletal proteins might also be important in their postsynaptic accumulation. For example, Shank interacts with α-fodrin (Böckers et al., 2001), cortactin (Hering and Sheng, 2003) and Abp1 (Qualmann et al., 2004), proteins that bind to F-actin. Homer proteins were also reported to bind F-actin (Shiraishi et al., 1999) and drebrin (Shiraishi-Yamaguchi et al., 2009). Interestingly, scaffolding proteins with mutations in their binding motifs to other PSD partners (for example disruption of GKAP–Shank interaction) can still be targeted to the postsynapse but are less stable and more dependent on F-actin, highlighting once again the importance of scaffold interactions with the cytoskeleton and emphasising the need to interact with scaffolding partners to stabilize the protein complexes in the PSD (Kuriu et al., 2006). In addition to its role in targeting of synaptic proteins to dendritic spines, GKAP–DLC2 interaction seems to stabilize the postsynaptic complex at the PSD. Indeed we showed that GKAP expression is no longer enhanced in spines upon neuronal activity in conditions of DLC2 overexpression (supplementary material Fig. S4). In these conditions, the activity-induced increase in GKAP–DLC2 interaction identified by BRET experiments highlights the importance of a local enhancement of GKAP–DLC2 interactions in spines (rather than accumulation of GKAP per se) to stabilize GKAP and PSD-95 in spines. This was further confirmed by the co-transfection experiment shown in Fig. 5B, which demonstrated that despite an increasing concentration in spines of a GKAP mutant that could not interact with DLC2 but could bind correctly to PSD-95 and Shank3, the absence of GKAP–DLC2 interaction within the spine impairs the stabilization of the scaffolding complex. This result highlights the role of DLC2 as a hub protein that interacts with partially disordered proteins to promote their adequate organization and stabilizes the scaffolding complex at the PSD.

Such a role of DLC2 has been previously described for other interactors, and this structuring feature was proposed to rely on the DLC2-induced promotion of protein dimerization (for a review, see Barbar, 2008). Whether DLC2 enables GKAP dimerization to stabilize functional protein complex in the PSD is currently under investigation.

The importance of GKAP–DLC2 interaction in the targeting and stabilization of synaptic proteins described here is physiologically relevant, as 4-AP-induced sustained synaptic activity enhanced GKAP–DLC2 interaction and synaptic proteins accumulation in the PSD. This result corroborates previous studies showing that treatment of neurons with bicuculline and 4-AP resulted in accumulation of GKAP and suppression of its dynamics in synapses (Kuriu et al., 2006). We found that activity-induced GKAP accumulation in spines required GKAP interaction with DLC2. However, the molecular mechanisms underlying the synaptic activity-dependent modulation of GKAP–DLC2 interaction and consequent scaffold stabilization are still unknown. Dimerization of DLC is required for its activity because the monomer lacks the groove that is necessary for binding (Liang et al., 1999; Wang et al., 2003). The DLC monomer–dimer equilibrium is controlled by electrostatic interactions at the dimer interface, such as by phosphorylation of Ser88, which is a regulatory mechanism for DLC in vivo (Benison et al., 2009). Enhanced synaptic activity might affect the balance between phosphatases and kinases activation, thus displacing DLC phosphorylation–dephosphorylation equilibrium and dimerization, which in turn would modulate its binding to molecular substrates such as GKAP. One interesting candidate is the p-21-activated kinase (PAK) family. Phosphorylation of DLC is an important regulatory mechanism in vivo because phosphorylation at Ser88 by Pak1 inhibits apoptosis and promotes cancerous phenotypes (Puthalakath et al., 1999; Song et al., 2008; Vadlamudi et al., 2004). In cultured hippocampal neurons, the active form phosphorylated PAK accumulates in puncta that colocalize with PSD-95 (Zhang et al., 2005). Whether this depends on synaptic activity and affects DLC–GKAP interaction remains to be investigated.

Our results suggest that an important functional consequence of postsynaptic scaffold stabilization of the DLC–GKAP complex is the upregulation of NMDA receptor-channel activity. Previous reports have described the clustering of NMDA receptors by PSD-95 at the surface of heterologous cells (Kornau et al., 1995; Lin et al., 2004; Niethammer et al., 1996), through inhibition of receptor internalization (Roche et al., 2001). In *Xenopus* oocytes, PSD-95 functionally increases NMDA currents, and GKAP markedly potentiates the channel activity of the receptor-PSD-95 complex (Yamada et al., 1999), suggesting that GKAP could make the signal transmission more efficient at postsynaptic sites. However, to date, despite a couple of studies suggesting that functional localization of NMDA receptors in synapses might depend on PSD-95 (for a review, see Kim and Sheng, 2004), the impact of PSD-95 and associated proteins on the regulation of NMDA currents in neurons remains largely unknown. Here, we demonstrated that the overall consequence of GKAP–DLC2 interaction in spines, and stabilization of GKAP and PSD-95 in the PSD is the potentiation of postsynaptic NMDA currents in hippocampal neurons. The role of GKAP–DLC2 interaction in organizing the postsynaptic scaffold complex could also affect AMPA receptor function. Indeed the transmembrane AMPA receptor regulatory proteins (TARPs) are important for the regulation of AMPA receptor activity at synapses. TARPS stabilize AMPA receptors at synapses through direct interactions with PSD-95 and other membrane associated guanylate kinases (Jackson and Nicoll, 2011). This interaction was shown to be necessary for synaptic AMPA receptor function by measuring AMPA-receptor-mediated excitatory post-synaptic currents (EPSCs) following PDZ-domain mutation (Schnell et al., 2002), and by acute disruption of the interaction between TARPs and PSD-95 using biomimetic divalent ligands (Sainlos et al., 2011). By increasing PSD-95 location in spines, GKAP–DLC2 interaction could therefore also controls AMPA receptor function.

Given that NMDA receptors are fundamental players involved in synaptic transmission, the mechanism identified in this study, of functional regulation of synaptic NMDA receptor activity by DLC2–GKAP interaction might be of physiological importance in synaptic plasticity. Impaired GKAP expression and abnormal NMDA-glutamatergic neurotransmission have been identified in psychiatric disorders, such as schizophrenia (Kajimoto et al., 2003), obsessive-compulsive disorder (Welch et al., 2007) and fragile X mental retardation (Schütt et al., 2009). It is worth examining whether GKAP–DLC2 assembly is associated with these disorders in order to validate the GKAP–DLC2 interaction as a new pharmacological target for the development of therapeutic compounds.

Materials and Methods

Plasmids and siRNA

The DLC2-pCMV-SPORT6 plasmid was purchased from Source BioScience Geneservice (Nottingham, UK). The Venus tag was added in frame with the 5′ end coding sequence of DLC2 using Gateway Technology (Invitrogen, Paisley, UK) to obtain the p-Venus-DLC2 plasmid. The coding sequence of Venus in p-Venus-DLC2 and mCherry were exchanged by molecular subcloning to obtain pmCherry-DLC2. siRNA raised against DLC2 (DYNLL2 siRNA mouse; Santa Cruz Biotechnologies, ref. sc-143208, Heidelberg, Germany) was a pool of three target-specific 19- to 25-base-pair siRNAs designed to knock down gene expression. The siRNA control was purchased from Invitrogen. The pAmCyan1-N1 vector was purchased from Clontech Laboratories (ref. 632442, Takara Bio Inc., Saint-Germain-en-Laye, France). The coding sequence of GKAP1a was a generous gift from Carlo Sala (Institute of Neuroscience, CNR, Milan, Italy). The coding sequence of CFP and RLuc8 were added in the 5′ end coding sequence of GKAP1a using Gateway Technology to obtain the p-CFP-GKAP1a and p-RLuc8-GKAP1a expression plasmids, respectively. From these two expression plasmids, we constructed p-CFP-GKAP1a-mutant and p-RLuc8-GKAP1a-mutant by using two successive primers containing point mutations: 5′-TCCAGTCCGTGGGAGT-GGAAGTAGAA-3′ and 5′-CTATCAATTGGGAATCAGAATGACGACGCCG-AAGAGTCA-3′. The coding sequence of Venus was added in frame with the 5′ end of the Shank3 coding sequence to obtain pRK5-Venus-Shank3. The PSD-95-YFP plasmid was a generous gift from Daniel Choquet (Institut interdisciplinaire de Neurosciences, Bordeaux, France).

Cell cultures and transfection

HEK293 cell culture and transfection were performed as previously described (Perroy et al., 2004). For BRET experiments, a constant quantity of the plasmid coding for the donor entity (50 ng) was combined with various quantities of the plasmid coding for the acceptor entity (–300 ng). The total amount of DNA per plate (100 nm diameter, 3,000,000 cells) was then complemented with the non-coding plasmid pcDNA3 to reach 5 μg of DNA in each transfection. For the co-immunoprecipitation experiments, we transfected 2.5 μg of each of the DNAs coding for the two proteins of interest per plate. Hippocampal neuronal primary cultures were prepared from embryonic day 17.5 mice and grown in neurobasal medium (Gibco, Invitrogen, Cergy Pontoise, France) supplemented with B-27 (Gibco, diluted at 1:50), glutamax (4 mM, Gibco), glutamic acid (25 μM, Gibco), antibiotics (100 IU/ml penicillin and 100 μg/ml streptomycin) and 10% fetal bovine serum (FBS). After 3 days in culture (DIV3), the culture medium was supplemented with cytosine β-D-arabinofuranoside hydrochloride 5 μM (Sigma-Aldrich, St Quentin Fallavier, France) for 12 hours. Then, 75% of the medium was replaced with neurobasal medium supplemented with B27, glutamax and antibiotics. Neurons were then transfected with expression plasmids or siRNAs at DIV11 using Lipofectamine 2000 (Invitrogen, Cergy

Pontoise, France) according to the manufacturer's standard protocol and studied between DIV12 and DIV14. The siRNAs were resuspended to a final concentration of 10 µM, and 3 µl of this solution were used for transfection in 35 mm diameter culture dishes.

BRET measurements

BRET is a very sensitive technology that in the past decade has become the technology of choice to study the dynamics of protein–protein interactions in living cells. The efficacy of the energy transfer depends on the close proximity (<10 nm) and orientation of the donor and acceptor entities. The average radius of proteins being 5 nm, the occurrence of resonance energy transfer is interpreted as a strong indication that the proteins attached to the energy donors and acceptors respectively are indeed in direct contact (Boute et al., 2002; Pfleger and Eidne, 2006). BRET measurements in cell populations were performed as previously described (Perroy et al., 2004). Single cell BRET imaging in cultured hippocampal neurons to study the subcellular localization of protein-protein interactions was performed according to previously published protocols (Coulon et al., 2008; Perroy, 2010). Briefly, images were obtained using a Plan-Apochromat 63×/1.40 oil M27 objective, at room temperature. Hippocampal neurons were transfected at DIV11 and recorded at DIV14 in the external medium used for electrophysiological recordings (see the following section). Transfected cells were first identified using a monochromatic light and appropriate filter to excite the Venus (exciter HQ480/40 #44001 – emitter HQ600/50 #42017, Chroma, Olching, Germany). The light source was then switched off until the end of the experiment. Coelenterazine H (CoelH, 20 µM) was applied for 5 minutes before acquisition with Metamorph software (Molecular Devices). Images were then collected using a cascade 512B camera from Photometrics. Sequential acquisitions of 30 seconds each were performed at 5 MHz (Gain 3950, binning 1) with emission filters D480/60 nm (#61274, Chroma) and HQ535/50 nm (#63944, Chroma) to select em480 and em535 wavelengths, respectively. The pixel-by-pixel 535 nm:480 nm ratios were calculated by dividing the absolute blue or yellow intensities per pixel of the images obtained at 535 nm over 480 nm. These numerical ratios (between 0 and 1.5) were translated and visualized with a continuous 256 pseudo-color look-up table (LUT) as displayed in the figures. To determine the average intensity and distribution of the 535 nm:480 nm fluorescence ratios, the mean intensity and standard deviation of pixels was calculated within a square region drawn on the cell of interest using ImageJ software (NIH). CoelH 20 µM was applied 5 minutes before the first BRET image acquisition, and 4-AP (or NMDA) was added immediately after the first acquisition. The sequential acquisitions were then performed from the 535 and 480 nm channels, 1, 5 and 10 minutes after the beginning of 4-AP (or NMDA) application.

Electrophysiological recordings and data analysis

Hippocampal neurons were recorded in the whole-cell patch-clamp configuration, using an Axopatch 200B amplifier. Currents were filtered at 1 kHz, digitized at 3 kHz and analyzed using pClamp 10.0 software (Axon Instruments; Molecular Devices, Sunnyvale, CA). Currents were recorded in DIV12–13 hippocampal neurons at room temperature, at a holding potential of −60 mV. The recording pipettes had a resistance of 3–7 MΩ.

For mEPSC recordings, pipettes were filled with the following medium: 140 mM KCl, 10 mM HEPES, 10 mM D-glucose, pH 7.2, with an osmolarity of 300 mOsm. Neurons were perfused continuously with the following external medium: 140 mM NaCl, 2 mM $CaCl_2$, 3 mM KCl, 10 mM HEPES, 10 mM D-glucose, 0.01 mM glycine, 0.01 mM bicuculline, 0.0003 mM tetrodotoxin, pH 7.4, with an osmolarity of 330 mOsm. Once a minimal sample of at least 20 mEPSCs had been collected from a neuron, the average amplitude of these events was measured on the total duration of the sample. The average trace was normalized and pooled with other average traces recorded in the same condition to obtain a single representative trace, thus allowing us to study the slow component (NMDA dependent) of the event. For NMDA current recordings, pipettes were filled with the following medium: 5 mM EGTA, 0.5 mM $CaCl_2$, 140 mM CsCl, 10 mM HEPES, 10 mM D-glucose, pH 7.2, with an osmolarity of 300 mOsm. Neurons were perfused continuously with the following external medium: 140 mM NaCl, 2 mM $CaCl_2$, 3 mM KCl, 10 mM HEPES, 10 mM D-glucose, 0.01 mM glycine, 0.0003 mM tetrodotoxin, pH 7.4, with an osmolarity of 330 mOsm. Whole-cell NMDA currents were evoked in neurons by 10-second applications of 100 µM NMDA (Sigma-Aldrich, St Quentin Fallavier, France). The agonist was applied three times at 60-second intervals, and the averaged peak current amplitude was then calculated from the three pharmacological stimulations. All electrophysiological data were analyzed using the Clampfit 10 software from Axon Instruments (Molecular Devices).

Immunoprecipitation and western blot analyses

Cells were lysed in 0.1% Triton X-100, 150 mM NaCl, 2 mM EGTA, anti-protease mixture (Roche Applied Science) and 20 mM Tris-HCl, pH 7.4 (lysis buffer), and the mixture was centrifuged. The lysate obtained from 10^7 cells transfected with mCherry–DLC2 and CFP–GKAP or CFP–GKAPmut was co-immunoprecipitated using RFP-Trap from ChromoTek (Planegg-Martinsried, Germany) according to the manufacturer's protocol (http://www.chromotek.com/downloads/RFP-Trap_A%20manual.pdf). The RFP-Trap, a small RFP binding protein coupled to agarose beads, enables purification of any protein of interest fused to RFP (monomeric derivates of DsRed, including mRFP1, mCherry, mPlum, mOrange). After extensive washing, the solid phase was incubated in Laemmli buffer at 90°C. A control assay was performed under the same conditions but with cells transfected with mCherry instead of mCherry–DLC2 and CFP–GKAP or CFP–GKAPmut. Protein samples were resolved by 7.5% PAGE, transferred to nitrocellulose, and subjected to immunoblotting using rabbit anti-GFP antibody (1:1000, Invitrogen) or anti-RFP (1:1000, MBL, Woburn, MA) for 1 hour. The blots were then washed three times with PBS containing 0.1% Tween 20 (PBST). The nitrocellulose was then incubated with goat anti-rabbit IgG DyLight™ 800 conjugated (Pierce, Thermo Fisher, Rockford, IL) for 1 hour. The blots were then washed three times with PBST. Proteins were visualized by scanning on an Odissey Infrared Imaging System (LI-COR Biosciences) with 800 nm channel. The total level of the three proteins DLC2, GKAP and GKAPmutant was determined to evaluate equal transfection efficiency. The ratio of immunoprecipitated proteins was quantified: CFP–GKAP/mCherry–DLC2 and CFP–GKAPmutant/mCherry–DLC2. To quantify the loss of interaction due to the mutation of GKAP, the ratio of CFP–GKAPmutant/mCherry–DLC2 was expressed as a percentage of the ratio CFP–GKAP/mCherry–DLC2.

To stain endogenous PSD-95, after fixation, cells were permeabilized with 0.15% Triton X-100 for 5 minutes, washed and incubated with a primary mouse monoclonal antibody raised against PSD95 (1:200, Santa Cruz) for 30 minutes at room temperature. Cells were washed and incubated with Cy3-conjugated secondary donkey anti-mouse IgG antibody (1:1000, Jackson Laboratory) for 1 hour at room temperature.

Immunocytochemistry

Hippocampal neurons were fixed at DIV12 in PBS containing 4% paraformaldehyde for 15 minutes at room temperature. Cells were then washed and mounted on coverslips with Moviol. To enhance synaptic activity, 1 mM 4-AP was added for –5 minutes and removed immediately before fixation, excepted for the experiments in Fig. 5C where neurons were washed 25 minutes before fixation in order to follow long lasting neuronal remodeling. Images were acquired using an Apotome microscope (axio Imager.Z1; Zeiss, Thornwood, NY). For quantification of the spine/shaft fluorescence ratio, the fluorescence intensity of spine and shaft was measured using ImageJ software. More than 100 spines were measured for each construct and each experiment was repeated at least three times in separate neuronal cultures.

Analysis of the transcript level of DLC2

Total RNA was extracted from hippocampal neurons with Trizol reagent (Invitrogen) according to the manufacturer's instructions. RT-PCR analysis of total RNA was carried out with random hexamer oligonucleotides for reverse transcription. Sequences of the primers used for the determination of DLC2 expression levels are: 5′-TCTGCGTTCTTGATCACTGC-3′ and 5′-TCCTGTTGCATGTCCTCAGA-3′. The level of expression of DLC2 was normalized to the geometric mean of the expression levels of three housekeeping genes (aldolase, *GAPDH, B2M*), according to the formula: X/geometric mean (R1, R2, R3)$=2^{(Ct[X]\text{-arithmetic mean }[Ct(R1),Ct(R2),Ct(R3)])}$, where Ct is the threshold cycle, and R1, R2, R3 the reference genes.

Acknowledgements

We thank Abhijit De and Andreas Loening for providing us the pcDNA3.1-*Rluc*8 plasmid. We thank Atsushi Miyawaki for providing the pcDNA3.1-Venus plasmid. We are grateful to Daniel Choquet and Carlo Sala for the kind gifts of PSD-95 and GKAP coding plasmids, respectively. BRET experiments on cell population were performed using the ARPEGE Pharmacology Screening Interactome platform facility at the Institute of Functional Genomics (Montpellier, France).

Funding

This work was supported by the European Community [Health-F2-2008-222918 - REPLACES to L.F.]; Agence Nationale de la Recherche [ANR-08-MNPS-037-01, SYNGEN to L.F., ANR-11-BSV4-018-03, DELTAPLAN to J.P.]; DIaTrAl FUI-EuroBioMed 2010 to L.F. and F.R.; and La fondation Jérôme Lejeune to E.M. and J.P.

References

Barbar, E. (2008). Dynein light chain LC8 is a dimerization hub essential in diverse protein networks. *Biochemistry* **47**, 503-508.

Benashski, S. E., Harrison, A., Patel-King, R. S. and King, S. M. (1997). Dimerization of the highly conserved light chain shared by dynein and myosin V. *J. Biol. Chem.* **272**, 20929-20935.

Benison, G., Chiodo, M., Karplus, P. A. and Barbar, E. (2009). Structural, thermodynamic, and kinetic effects of a phosphomimetic mutation in dynein light chain LC8. *Biochemistry* **48**, 11381-11389.

Böckers, T. M., Mameza, M. G., Kreutz, M. R., Bockmann, J., Weise, C., Buck, F., Richter, D., Gundelfinger, E. D. and Kreienkamp, H. J. (2001). Synaptic scaffolding proteins in rat brain. Ankyrin repeats of the multidomain Shank protein family interact with the cytoskeletal protein alpha-fodrin. *J. Biol. Chem.* **276**, 40104-40112.

Boeckers, T. M., Winter, C., Smalla, K. H., Kreutz, M. R., Bockmann, J., Seidenbecher, C., Garner, C. C. and Gundelfinger, E. D. (1999). Proline-rich synapse-associated proteins ProSAP1 and ProSAP2 interact with synaptic proteins of the SAPAP/GKAP family. *Biochem. Biophys. Res. Commun.* **264**, 247-252.

Boute, N., Jockers, R. and Issad, T. (2002). The use of resonance energy transfer in high-throughput screening: BRET versus FRET. *Trends Pharmacol. Sci.* **23**, 351-354.

Buckle, P. J. and Haas, H. L. (1982). Enhancement of synaptic transmission by 4-aminopyridine in hippocampal slices of the rat. *J. Physiol.* **326**, 109-122.

Coulon, V., Audet, M., Homburger, V., Bockaert, J., Fagni, L., Bouvier, M. and Perroy, J. (2008). Subcellular imaging of dynamic protein interactions by bioluminescence resonance energy transfer. *Biophys. J.* **94**, 1001-1009.

Dick, T., Ray, K., Salz, H. K. and Chia, W. (1996). Cytoplasmic dynein (ddlc1) mutations cause morphogenetic defects and apoptotic cell death in Drosophila melanogaster. *Mol. Cell. Biol.* **16**, 1966-1977.

Echeverri, C. J., Paschal, B. M., Vaughan, K. T. and Vallee, R. B. (1996). Molecular characterization of the 50-kD subunit of dynactin reveals function for the complex in chromosome alignment and spindle organization during mitosis. *J. Cell Biol.* **132**, 617-633.

Ehlers, M. D., Mammen, A. L., Lau, L. F. and Huganir, R. L. (1996). Synaptic targeting of glutamate receptors. *Curr. Opin. Cell Biol.* **8**, 484-489.

Ehrlich, I. and Malinow, R. (2004). Postsynaptic density 95 controls AMPA receptor incorporation during long-term potentiation and experience-driven synaptic plasticity. *J. Neurosci.* **24**, 916-927.

Fejtova, A., Davydova, D., Bischof, F., Lazarevic, V., Altrock, W. D., Romorini, S., Schöne, C., Zuschratter, W., Kreutz, M. R., Garner, C. C. et al. (2009). Dynein light chain regulates axonal trafficking and synaptic levels of Bassoon. *J. Cell Biol.* **185**, 341-355.

Fuhrmann, J. C., Kins, S., Rostaing, P., El Far, O., Kirsch, J., Sheng, M., Triller, A., Betz, H. and Kneussel, M. (2002). Gephyrin interacts with Dynein light chains 1 and 2, components of motor protein complexes. *J. Neurosci.* **22**, 5393-5402.

Gerrow, K., Romorini, S., Nabi, S. M., Colicos, M. A., Sala, C. and El-Husseini, A. (2006). A preformed complex of postsynaptic proteins is involved in excitatory synapse development. *Neuron* **49**, 547-562.

Hering, H. and Sheng, M. (2003). Activity-dependent redistribution and essential role of cortactin in dendritic spine morphogenesis. *J. Neurosci.* **23**, 11759-11769.

Hirao, K., Hata, Y., Ide, N., Takeuchi, M., Irie, M., Yao, I., Deguchi, M., Toyoda, A., Sudhof, T. C. and Takai, Y. (1998). A novel multiple PDZ domain-containing molecule interacting with N-methyl-D-aspartate receptors and neuronal cell adhesion proteins. *J. Biol. Chem.* **273**, 21105-21110.

Jackson, A. C. and Nicoll, R. A. (2011). The expanding social network of ionotropic glutamate receptors: TARPs and other transmembrane auxiliary subunits. *Neuron* **70**, 178-199.

Jaffrey, S. R. and Snyder, S. H. (1996). PIN: an associated protein inhibitor of neuronal nitric oxide synthase. *Science* **274**, 774-777.

Kaiser, F. J., Tavassoli, K., Van den Bemd, G. J., Chang, G. T., Horsthemke, B., Möröy, T. and Lüdecke, H. J. (2003). Nuclear interaction of the dynein light chain LC8a with the TRPS1 transcription factor suppresses the transcriptional repression activity of TRPS1. *Hum. Mol. Genet.* **12**, 1349-1358.

Kajimoto, Y., Shirakawa, O., Lin, X. H., Hashimoto, T., Kitamura, N., Murakami, N., Takumi, T. and Maeda, K. (2003). Synapse-associated protein 90/postsynaptic density-95-associated protein (SAPAP) is expressed differentially in phencyclidine-treated rats and is increased in the nucleus accumbens of patients with schizophrenia. *Neuropsychopharmacology* **28**, 1831-1839.

Kennedy, M. B. (1997). The postsynaptic density at glutamatergic synapses. *Trends Neurosci.* **20**, 264-268.

Kim, E. and Sheng, M. (2004). PDZ domain proteins of synapses. *Nat. Rev. Neurosci.* **5**, 771-781.

Kim, E., Naisbitt, S., Hsueh, Y. P., Rao, A., Rothschild, A., Craig, A. M. and Sheng, M. (1997). GKAP, a novel synaptic protein that interacts with the guanylate kinase-like domain of the PSD-95/SAP90 family of channel clustering molecules. *J. Cell Biol.* **136**, 669-678.

King, S. M. and Patel-King, R. S. (1995). The M(r) = 8,000 and 11,000 outer arm dynein light chains from Chlamydomonas flagella have cytoplasmic homologues. *J. Biol. Chem.* **270**, 11445-11452.

King, S. M., Barbarese, E., Dillman, J. F., 3rd, Patel-King, R. S., Carson, J. H. and Pfister, K. K. (1996). Brain cytoplasmic and flagellar outer arm dyneins share a highly conserved Mr 8,000 light chain. *J. Biol. Chem.* **271**, 19358-19366.

Kornau, H. C., Schenker, L. T., Kennedy, M. B. and Seeburg, P. H. (1995). Domain interaction between NMDA receptor subunits and the postsynaptic density protein PSD-95. *Science* **269**, 1737-1740.

Kuriu, T., Inoue, A., Bito, H., Sobue, K. and Okabe, S. (2006). Differential control of postsynaptic density scaffolds via actin-dependent and -independent mechanisms. *J. Neurosci.* **26**, 7693-7706.

Lajoix, A. D., Gross, R., Aknin, C., Dietz, S., Granier, C. and Laune, D. (2004). Cellulose membrane supported peptide arrays for deciphering protein-protein interaction sites: the case of PIN, a protein with multiple natural partners. *Mol. Divers.* **8**, 281-290.

Lee, K. H., Lee, S., Kim, B., Chang, S., Kim, S. W., Paick, J. S. and Rhee, K. (2006). Dazl can bind to dynein motor complex and may play a role in transport of specific mRNAs. *EMBO J.* **25**, 4263-4270.

Liang, J., Jaffrey, S. R., Guo, W., Snyder, S. H. and Clardy, J. (1999). Structure of the PIN/LC8 dimer with a bound peptide. *Nat. Struct. Biol.* **6**, 735-740.

Lin, Y., Skeberdis, V. A., Francesconi, A., Bennett, M. V. and Zukin, R. S. (2004). Postsynaptic density protein-95 regulates NMDA channel gating and surface expression. *J. Neurosci.* **24**, 10138-10148.

Lo, K. W., Naisbitt, S., Fan, J. S., Sheng, M. and Zhang, M. (2001). The 8-kDa dynein light chain binds to its targets via a conserved (K/R)XTQT motif. *J. Biol. Chem.* **276**, 14059-14066.

Lo, K. W., Kan, H. M., Chan, L. N., Xu, W. G., Wang, K. P., Wu, Z., Sheng, M. and Zhang, M. (2005). The 8-kDa dynein light chain binds to p53-binding protein 1 and mediates DNA damage-induced p53 nuclear accumulation. *J. Biol. Chem.* **280**, 8172-8179.

Lu, W., Man, H., Ju, W., Trimble, W. S., MacDonald, J. F. and Wang, Y. T. (2001). Activation of synaptic NMDA receptors induces membrane insertion of new AMPA receptors and LTP in cultured hippocampal neurons. *Neuron* **29**, 243-254.

Naisbitt, S., Kim, E., Weinberg, R. J., Rao, A., Yang, F. C., Craig, A. M. and Sheng, M. (1997). Characterization of guanylate kinase-associated protein, a postsynaptic density protein at excitatory synapses that interacts directly with postsynaptic density-95/synapse-associated protein 90. *J. Neurosci.* **17**, 5687-5696.

Naisbitt, S., Kim, E., Tu, J. C., Xiao, B., Sala, C., Valtschanoff, J., Weinberg, R. J., Worley, P. F. and Sheng, M. (1999). Shank, a novel family of postsynaptic density proteins that binds to the NMDA receptor/PSD-95/GKAP complex and cortactin. *Neuron* **23**, 569-582.

Naisbitt, S., Valtschanoff, J., Allison, D. W., Sala, C., Kim, E., Craig, A. M., Weinberg, R. J. and Sheng, M. (2000). Interaction of the postsynaptic density-95/guanylate kinase domain-associated protein complex with a light chain of myosin-V and dynein. *J. Neurosci.* **20**, 4524-4534.

Navarro, C., Puthalakath, H., Adams, J. M., Strasser, A. and Lehmann, R. (2004). Egalitarian binds dynein light chain to establish oocyte polarity and maintain oocyte fate. *Nat. Cell Biol.* **6**, 427-435.

Navarro-Lérida, I., Martínez Moreno, M., Roncal, F., Gavilanes, F., Albar, J. P. and Rodríguez-Crespo, I. (2004). Proteomic identification of brain proteins that interact with dynein light chain LC8. *Proteomics* **4**, 339-346.

Niethammer, M., Kim, E. and Sheng, M. (1996). Interaction between the C terminus of NMDA receptor subunits and multiple members of the PSD-95 family of membrane-associated guanylate kinases. *J. Neurosci.* **16**, 2157-2163.

Palay, S. L. (1958). The morphology of synapses in the central nervous system. *Exp. Cell Res.* **14 Suppl. 5**, 275-293.

Perroy, J. (2010). Subcellular dynamic imaging of protein-protein interactions in live cells by bioluminescence resonance energy transfer. *Methods Mol. Biol.* **591**, 325-333.

Perroy, J., Pontier, S., Charest, P. G., Aubry, M. and Bouvier, M. (2004). Real-time monitoring of ubiquitination in living cells by BRET. *Nat. Methods* **1**, 203-208.

Pfleger, K. D. and Eidne, K. A. (2006). Illuminating insights into protein-protein interactions using bioluminescence resonance energy transfer (BRET). *Nat. Methods* **3**, 165-174.

Puthalakath, H., Huang, D. C., O'Reilly, L. A., King, S. M. and Strasser, A. (1999). The proapoptotic activity of the Bcl-2 family member Bim is regulated by interaction with the dynein motor complex. *Mol. Cell* **3**, 287-296.

Puthalakath, H., Villunger, A., O'Reilly, L. A., Beaumont, J. G., Coultas, L., Cheney, R. E., Huang, D. C. and Strasser, A. (2001). Bmf: a proapoptotic BH3-only protein regulated by interaction with the myosin V actin motor complex, activated by anoikis. *Science* **293**, 1829-1832.

Qualmann, B., Boeckers, T. M., Jeromin, M., Gundelfinger, E. D. and Kessels, M. M. (2004). Linkage of the actin cytoskeleton to the postsynaptic density via direct interactions of Abp1 with the ProSAP/Shank family. *J. Neurosci.* **24**, 2481-2495.

Raux, H., Flamand, A. and Blondel, D. (2000). Interaction of the rabies virus P protein with the LC8 dynein light chain. *J. Virol.* **74**, 10212-10216.

Roche, K. W., Standley, S., McCallum, J., Dune Ly, C., Ehlers, M. D. and Wenthold, R. J. (2001). Molecular determinants of NMDA receptor internalization. *Nat. Neurosci.* **4**, 794-802.

Sainlos, M., Tigaret, C., Poujol, C., Olivier, N. B., Bard, L., Breillat, C., Thiolon, K., Choquet, D. and Imperiali, B. (2011). Biomimetic divalent ligands for the acute disruption of synaptic AMPAR stabilization. *Nat. Chem. Biol.* **7**, 81-91.

Scannevin, R. H. and Huganir, R. L. (2000). Postsynaptic organization and regulation of excitatory synapses. *Nat. Rev. Neurosci.* **1**, 133-141.

Schnell, E., Sizemore, M., Karimzadegan, S., Chen, L., Bredt, D. S. and Nicoll, R. A. (2002). Direct interactions between PSD-95 and stargazin control synaptic AMPA receptor number. *Proc. Natl. Acad. Sci. USA* **99**, 13902-13907.

Schnorrer, F., Bohmann, K. and Nüsslein-Volhard, C. (2000). The molecular motor dynein is involved in targeting swallow and bicoid RNA to the anterior pole of Drosophila oocytes. *Nat. Cell Biol.* **2**, 185-190.

Schütt, J., Falley, K., Richter, D., Kreienkamp, H. J. and Kindler, S. (2009). Fragile X mental retardation protein regulates the levels of scaffold proteins and glutamate receptors in postsynaptic densities. *J. Biol. Chem.* **284**, 25479-25487.

Sheng, M. and Pak, D. T. (2000). Ligand-gated ion channel interactions with cytoskeletal and signaling proteins. *Annu. Rev. Physiol.* **62**, 755-778.

Shiraishi, Y., Mizutani, A., Bito, H., Fujisawa, K., Narumiya, S., Mikoshiba, K. and Furuichi, T. (1999). Cupidin, an isoform of Homer/Vesl, interacts with the actin cytoskeleton and activated rho family small GTPases and is expressed in developing mouse cerebellar granule cells. *J. Neurosci.* **19**, 8389-8400.

Shiraishi-Yamaguchi, Y., Sato, Y., Sakai, R., Mizutani, A., Knöpfel, T., Mori, N., Mikoshiba, K. and Furuichi, T. (2009). Interaction of Cupidin/Homer2 with two actin cytoskeletal regulators, Cdc42 small GTPase and Drebrin, in dendritic spines. *BMC Neurosci.* **10**, 25.

Sodeik, B., Ebersold, M. W. and Helenius, A. (1997). Microtubule-mediated transport of incoming herpes simplex virus 1 capsids to the nucleus. *J. Cell Biol.* **136**, 1007-1021.

Song, C., Wen, W., Rayala, S. K., Chen, M., Ma, J., Zhang, M. and Kumar, R. (2008). Serine 88 phosphorylation of the 8-kDa dynein light chain 1 is a molecular switch for its dimerization status and functions. *J. Biol. Chem.* **283**, 4004-4013.

Stein, V., House, D. R., Bredt, D. S. and Nicoll, R. A. (2003). Postsynaptic density-95 mimics and occludes hippocampal long-term potentiation and enhances long-term depression. *J. Neurosci.* **23**, 5503-5506.

Takeuchi, M., Hata, Y., Hirao, K., Toyoda, A., Irie, M. and Takai, Y. (1997). SAPAPs. A family of PSD-95/SAP90-associated proteins localized at postsynaptic density. *J. Biol. Chem.* **272**, 11943-11951.

Tu, J. C., Xiao, B., Naisbitt, S., Yuan, J. P., Petralia, R. S., Brakeman, P., Doan, A., Aakalu, V. K., Lanahan, A. A., Sheng, M. et al. (1999). Coupling of mGluR/Homer and PSD-95 complexes by the Shank family of postsynaptic density proteins. *Neuron* **23**, 583-592.

Vadlamudi, R. K., Bagheri-Yarmand, R., Yang, Z., Balasenthil, S., Nguyen, D., Sahin, A. A., den Hollander, P. and Kumar, R. (2004). Dynein light chain 1, a p21-activated kinase 1-interacting substrate, promotes cancerous phenotypes. *Cancer Cell* **5**, 575-585.

Wang, W., Lo, K. W., Kan, H. M., Fan, J. S. and Zhang, M. (2003). Structure of the monomeric 8-kDa dynein light chain and mechanism of the domain-swapped dimer assembly. *J. Biol. Chem.* **278**, 41491-41499.

Welch, J. M., Lu, J., Rodriguiz, R. M., Trotta, N. C., Peca, J., Ding, J. D., Feliciano, C., Chen, M., Adams, J. P., Luo, J. et al. (2007). Cortico-striatal synaptic defects and OCD-like behaviours in Sapap3-mutant mice. *Nature* **448**, 894-900.

Yamada, Y., Chochi, Y., Ko, J. A., Sobue, K. and Inui, M. (1999). Activation of channel activity of the NMDA receptor-PSD-95 complex by guanylate kinase-associated protein (GKAP). *FEBS Lett.* **458**, 295-298.

Yang, Z., Vadlamudi, R. K. and Kumar, R. (2005). Dynein light chain 1 phosphorylation controls macropinocytosis. *J. Biol. Chem.* **280**, 654-659.

Zhang, H., Webb, D. J., Asmussen, H., Niu, S. and Horwitz, A. F. (2005). A GIT1/PIX/Rac/PAK signaling module regulates spine morphogenesis and synapse formation through MLC. *J. Neurosci.* **25**, 3379-3388.